Organic & Biomolecular Chemistry

Accepted Manuscript

This article can be cited before page numbers have been issued, to do this please use: O. Tietz, J. Kaur, A. Bhardwaj and F. Wuest, *Org. Biomol. Chem.*, 2016, DOI: 10.1039/C6OB00493H.

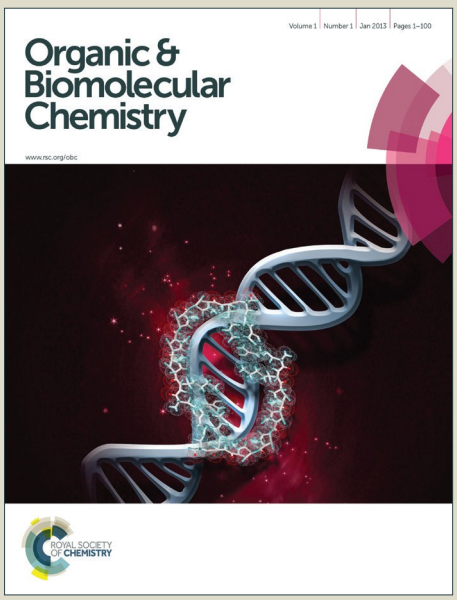

ROYAL SOCIETY OF CHEMISTRY

www.rsc.org/obc

View Article Online
DOI: 10.1039/C6OB00493H

Pyrimidine-based fluorescent COX-2 inhibitors: Synthesis and biological evaluation

Ole Tietz[a,1] Jatinder Kaur[a,b,1] Atul Bhardwaj[a,b]; Frank R. Wuest[*a,b]

[a]Department of Oncology, Cross Cancer Institute, University of Alberta, 11560 University Avenue, T6G 1Z2, Edmonton, AB, Canada.

[b]Department of Pharmacy and Pharmaceutical Sciences, Medical Sciences Building, University of Alberta, T6G 2H1, Edmonton, AB, Canada.

[1] Ole Tietz and Jatinder Kaur equally contributed to this work.

CORRESPONDING AUTHOR: Frank Wuest, Department of Oncology, Cross Cancer Institute, University of Alberta, 11560 University Avenue, Edmonton, AB, T6G 1Z2, Canada

Email: wuest@ualberta.ca

Telephone: 780 989 8150

Fax: 780-432-8483

EMAIL:

Ole Tietz – ole@ualberta.ca

Jatinder Kaur – kaur2@ualberta.ca

Atul Bhardwaj – abhardwa@ualberta.ca

Frank Wuest – wuest@ualberta.ca

View Article Online
DOI: 10.1039/C6OB00493H

ABSTRACT

The cyclooxygenase-2 (COX-2) enzyme is overexpressed in a variety of cancers and mediates inflammatory processes that aid the growth and progression of malignancies. Three novel and selective fluorescent COX-2 inhibitors have been designed and synthesized on the basis of previously reported pyrimidine-based COX-2 inhibitors and the 7-nitrobenzofurazan fluorophore. *In vitro* evaluation of COX-1/COX-2 isozyme inhibition identified *N*-(2-((7-nitro-benzo[c][1,2,5]oxadiazol-4-yl)amino)propyl)-4-[4-(methylsulfonyl)phenyl]-6-(trifluoro-methyl)-pyrimidin-2-amine (**6**) as novel potent and selective COX-2 inhibitor (IC_{50} = 1.8 μM). Lead compound (**6**) was further evaluated for its ability to selectively visualize COX-2 isozyme in COX-2 expressing human colon cancer cell line HCA-7 using confocal microscopy experiments.

View Article Online
DOI: 10.1039/C6OB00493H

INTRODUCTION

Cancer remains one of the most prevalent causes of death in the western world and contributes substantially to the pressure on healthcare systems worldwide. Despite significant advances in survival rates over the past decades, many therapeutic and diagnostic challenges of cancer remain. Inflammatory processes have been of constant interest in cancer research following their inclusion as one of the hallmarks of cancer.[1] Inflammation is of particular interest since it has been shown to enable and cause cancer. Inflammatory conditions are known to aid the development of tumors and act as a primary cause for cancer. A prominent example is inflammatory bowl disease which can lead to the development of colorectal cancer. More recently it was discovered that certain cancers develop inflammatory conditions in their tumor microenvironment even though there is no pathological basis for inflammation, indicating that inflammation is a driver for carcinogenesis. Inflammatory conditions were shown to influence cell proliferation and cell survival, angiogenesis, tumor cell migration and metastasis leading to tumor growth, progression and metastasis.[2] Tools that enable researchers to study biochemical mechanisms that initiate and sustain inflammatory responses *in vivo* would be of great value in the field of cancer research and advance our understanding of the multiple roles inflammation plays in the development and progression of cancer.

The cyclooxygenase enzyme family consists of two members: cyclooxygenase-1 (COX-1) and cyclooxygenase-2 (COX-2). COX enzymes control the initial step within the prostaglandin pathway by converting arachidonic acid to prostaglandin H_2 (PGH_2). PGH_2 is the primary substrate for the synthesis of a variety of prostaglandin signaling molecules, which are employed as autocrine and paracrine messengers to mediate a number of physiological and pathophysiological processes through binding to their respective G-protein coupled receptors. COX-1 is constitutively expressed in most resting tissues, while COX-2 is an inducible COX isoform and virtually absent in healthy tissues. COX-1 maintains tissue homeostasis and is primarily responsible for gastrointestinal and renal integrity.[3] COX-2 is expressed in response to pro-inflammatory stimuli and its expression is usually transient.[4] COX-2 is responsible for the production of inflammatory prostaglandins, which ultimately induce inflammation, pain and fever. Consequently, COX-2 is one of the most important therapeutic targets for the treatment of this pathological conditions.[5]

View Article Online
DOI: 10.1039/C6OB00493H

However, in view of cardiovascular safety concerns posed by most selective COX-2 inhibitors previously in clinical use, recent research efforts were focused on the development of nitric oxide releasing NSAIDs and dual COX/LOX inhibitors.[6-8]

COX-2 was shown to be upregulated in many human cancers, including gastric, lung, colon, esophageal and prostate carcinomas.[9-12] As a result, a number of COX-2 inhibitors have been investigated as anticancer agents [13-15] and some were shown to retard or prevent the progression of colon carcinomas.[16-18] The central role which COX-2 plays in the initiation and regulation of inflammatory processes, and the observed overexpression of COX-2 in a variety of cancers represent the rational for targeting the enzyme for cancer diagnosis and therapy. This perspective has led to the development of various radioactive positron emission tomography (PET) radiopharmaceuticals for the assessment of COX-2 expression *in vivo*.[19-21] Radiolabeled COX-2 inhibitors are ideally suited to study inflammation *in vivo*, but require laborious and expensive synthesis on a daily basis, due to their short half-live.

Fluorescence imaging agents on the other hand are cheaper, easier to prepare and have a longer shelf-live. Advances in chemistry and biological application of optical imaging probes have extensively been reviewed.[22-23] Fluorescent-labeled COX-2 inhibitors are suitable optical probes for the detection of COX-2 in cells and animals. Furthermore, they can be used for clinical imaging of tissues suitable for topical and endoluminal illumination such as esophagus and colon. A number of research groups are actively engaged in the design and synthesis of novel fluorescent-labeled COX-2 inhibitors.[24-26] Recently, our lab presented a highly selective celecoxib derivative conjugated with a 7-nitrobenzofurazan fluorophore (Celecoxib-NBD).[27] Celecoxib-NBD showed high affinity for COX-2 (IC_{50} = 0.19 μM) and a good selectivity profile over COX-1 (SI = 443). Furthermore, the fluorescence conjugate showed specific uptake in COX-2 positive HCA-7 cells while no uptake was observed in COX-2 negative HCT-116 cells, indicating that celecoxib-NBD is COX-2 specific *in vitro*. This work further showed that the NBD fluorophore is especially suitable for COX-2 targeting. Previous studies using celecoxib-rhodamine B conjugates showed lower affinity (IC_{50} = 3.9 μM) compared to celecoxib-NBD and reduced success in *in vitro* assays.[25]

View Article Online
DOI: 10.1039/C6OB00493H

Another research direction in our lab led to the development of a set of pyrimidine based COX-2 inhibitors to be used as short-lived PET radiotracers for molecular imaging.[30] Best inhibitors in the compound library showed inhibitory potencies for COX-2 greater than inhibitory potencies displayed by celecoxib in the same assay (IC_{50} = 5 nM versus IC_{50} = 40 nM).

In the present study we designed and developed a fluorescent COX-2 imaging probe (**6**) by using previously reported pyricoxib as lead structure (Figure 1).[28]

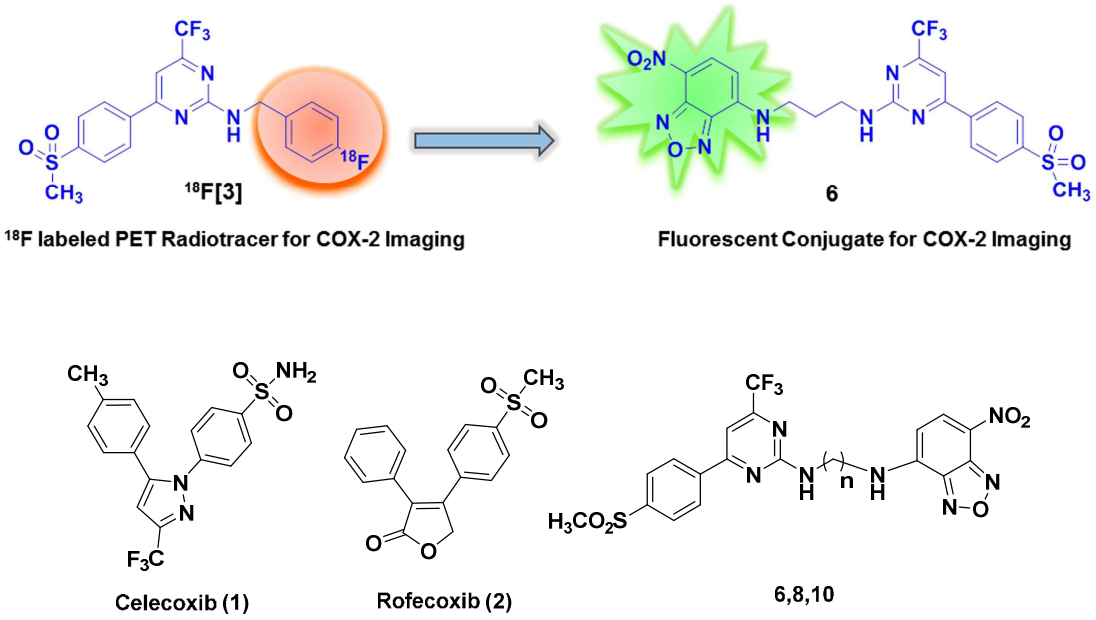

Figure 1. (Top) Design principle for fluorescent-labeled COX-2 inhibitors based on PET imaging radiotracers. (Bottom) Structures of celecoxib (**1**), rofecoxib (**2**), ^{18}F-labelled radiotracer (**[^{18}F]3**), and NBD-labeled compounds (**6, 8, 10**)

As part of our ongoing research program focused on molecular imaging of COX-2 in cancer,[27-30] we now describe *(i)* the synthesis of pyrimidine-based fluorescent conjugates (**6, 8, 10)** and their evaluation as *(ii) in vitro* COX-1 and COX-2 enzyme inhibitors, and their suitability as *(iii)* fluorescence imaging agents for the selective visualization of COX-2 activity in COX-2 expressing human colon cancer cell line HCA-7.

View Article Online
DOI: 10.1039/C6OB00493H

RESULTS AND DISCUSSION

Chemistry

The synthesis of NBD-labeled compounds **6**, **8** and **10** is illustrated in Scheme 1.

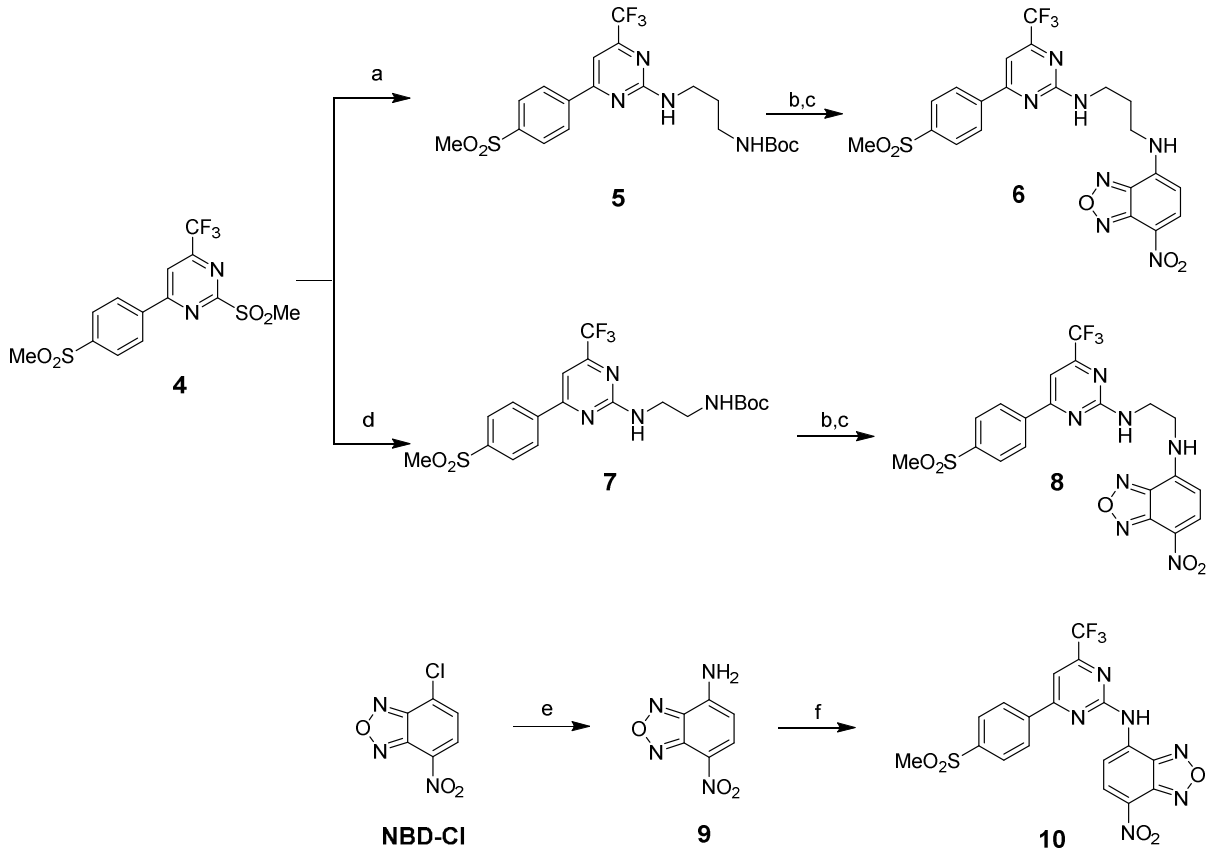

Scheme 1. *Reagents and conditions*: (a) *N*-Boc-propylenediamine, CH_3CN, 140 ^oC, 2 h; (b) TFA, dry CH_2Cl_2, 25 ^oC, 6 h; (c) NBD-Cl, dry TEA, dry THF, inert atmosphere, 25 ^oC, 2 h; (d) *N*-Boc-ethylenediamine, CH_3CN, 140 ^oC, 2 h; (e) NH_4OH solution (30 % in H_2O), CH_3OH, 25 ^oC, 18 h; (f) compound **4**, CH_3CN, 140 ^oC, 2 h.

4-Chloro-7-nitro-1,2,3-benzoxadiazole (NBD-chloride) was used to synthesize fluorescent pyrimidine scaffolds based on previously reported selective COX-2 inhibitor pyricoxib.[28,31] The use of NBD as a fluorophore for COX-2 imaging is well established, and the synthetic strategy used to develop fluorescent compounds **6**, **8** and **10** is similar to methods previously developed in our lab.[25,27]

View Article Online
DOI: 10.1039/C6OB00493H

Reaction of previously reported building block 2-(methylsulfonyl)-4-(4-(methylsulfonyl)-phenyl)-6-(trifluoromethyl)pyrimidine (**4**)[28,31] with *N*-Boc-propylenediamine or *N*-Boc-ethylenediamine in acetonitrile furnished the respective Boc-protected amines **5** and **7** in 58% and 64% yield, respectively.

Removal of the Boc protecting groups in compounds **5** and **7** by treatment with trifluoroacetic acid (TFA) in dry dichloromethane at 25 °C afforded the respective amine products, which were allowed to react with NBD-chloride without further purification. The NBD-conjugates **6** and **8** were synthesized in the presence of dry triethylamine (TEA) in dry THF in nitrogen atmosphere and underwent extensive purification by silica column chromatography and HPLC to obtain the final products in 25% (compound **6**) and 17% (compound **8**). The synthesis of compound **10** was accomplished by converting NBD-chloride into the primary amine compound **9** using ammonium hydroxide solution in methanol and water. The resulting 4-amino-7-nitrobenzofurazan (**9**) was reacted with building block (**4**) in acetonitrile and purified by silica column chromatography to give product **10** in 54% yield as a yellow solid.

COX-1 and COX-2 inhibition studies

Compounds (**6, 8** and **10**) were evaluated for their *in vitro* COX-1/COX-2 isozyme inhibitory potencies. The results are summarized in Table 1.

Table 1. *In vitro* COX-1 and COX-2 isozyme inhibition data.

Compound	IC_{50} (μM)[a]		COX-2 (SI)[b]
	COX-1	COX-2	
6	>100	1.8	>55.5
8	>100	6.0	>16.6
10	>100	4.6	>21.7
3	>100	0.007	>14285.7
1 (celecoxib)	7.7	0.04	192

[a] In vitro concentration of tested compound required to produce 50% inhibition of ovine COX-1 or human recombinant COX-2; results are the average of two determinations acquired using a COX fluorescence inhibitor assay (Cayman Chemical, Ann Arbor, USA; catalog #: 700100), and the deviation from the mean is <10% of the mean value. [b] In vitro COX-2 selectivity index (COX-1 IC_{50}/COX-2 IC_{50}).

View Article Online
DOI: 10.1039/C6OB00493H

In vitro COX-1/COX-2 inhibition studies showed that all three tested compounds (**6, 8** and **10**) are more potent inhibitors of COX-2 isoenzyme (IC_{50} = 1.8-6.0 μM range) than for COX-1 (IC_{50} = >100 μM). Among all three NBD-labeled compounds **6**, **8** and **10**, compound **6** containing a propylamino spacer between the NBD aryl ring and the pyrimidine moiety showed best COX-2 inhibitory potency and selectivity profile (COX-2 IC_{50} = 1.8 μM, SI = >55.5) compared to compounds containing a shorter (compound **8**) or no spacer (compound **10**). However, inhibitory potency of compound **6** against COX-2 isozyme is sunstantially lower compared to that of previously reported pyricoxib (COX-2 IC_{50} = 0.007 μM) and fluorescent-labeled celecoxib-NBD compound (COX-2 IC_{50} = 0.19 μM). In comparison to compound **6**, compound **8** (COX-2 IC_{50} = 6.0 μM) and **10** (COX-2 IC_{50} = 4.6 μM) were identified as less potent COX-2 inhibitors.

In contrast to our earlier work with celecoxib-NBD, where the NBD fluorophore was attached to structurally unaltered celecoxib at the sulfonamide moiety, here we did alter the structure of previously reported pyricoxib (**3**). The fluorophore was inserted to replace the 4-fluorobenzyl moiety rather than attached to an "intact" anti-inflammatory drug as previously reported.[24-27] Our aim was to synthesize a small fluorescence conjugate that could achieve deeper penetration into the COX-2 binding pocket due to reduced steric bulk. Compound **10** was designed to meet this specification, where the 4-fluorobenzyl moiety is replaced with similar sized nitro-benzoxadiazole moiety. However, the resulting compounds showed a substantial decrease in COX-2 inhibitory potency (from compound **3** COX-2 IC_{50} = 0.007 μM to compound **10** COX-2 IC_{50} = 4.6 μM). We have recently shown that a modest increase in steric bulk at 4-fluorobenzyl position in pyricoxib, by replacing fluorine with a phenyl, *tert*.-butyl or iodine group, had a substantial negative impact on binding affinity.[28,30] Molecular docking studies subsequently showed that the increased size of iodine lead the substituted benzyl flip into the complete opposite direction with lead to a less favorable interaction.[30] It is likely that the nitro-benzoxadiazole group is similarly reoriented in the binding pocket causing a loss of affinity.

View Article Online
DOI: 10.1039/C6OB00493H

***Fluorescence imaging of COX-2 expression in HCA-7 colon cancer cells*:**

From the three fluorescent conjugates (**6**, **8** and **10**), compound **6** was selected for further investigation using a fluorescence imaging experiment on COX-2-expressing human colon cancer HCA-7 cells. 4,6-Diamidino-2-phenylindole (DAPI) was used as a nucleus-specific stain. HCA-7 cells were incubated with compound **6** (100 μM) at 37 ^{o}C and cells were imaged by confocal microscopy. Cellular uptake of compound **6** was observed in COX-2 overexpressing HCA-7 cells (Figure 2b–d). Cells incubated with phosphate-buffered saline (PBS) under similar experimental conditions showed no fluorescence staining (Figure 2a). Pretreatment of HCA-7 cells with the potent and selective COX-2 inhibitor celecoxib (**1**, 5 μM) prevented all uptake of fluorescence conjugate (**6**) and no fluorescence labeling of the COX-2 isozyme was observed, which indicates that celecoxib is able to blocked the COX-2 binding of compound **6** in HCA-7 cells (Figure 2e). We performed the COX-2 fluorescence imaging experiment with compound **6** at different concentrations (1 μM, 50 μM, 100 μM, 200 μM and 500 μM). The results of these experiments indicate that COX-2 upregulation in HCA-7 cells is best visualized upon incubation of compound **6** at 100 μM concentration.

View Article Online
DOI: 10.1039/C6OB00493H

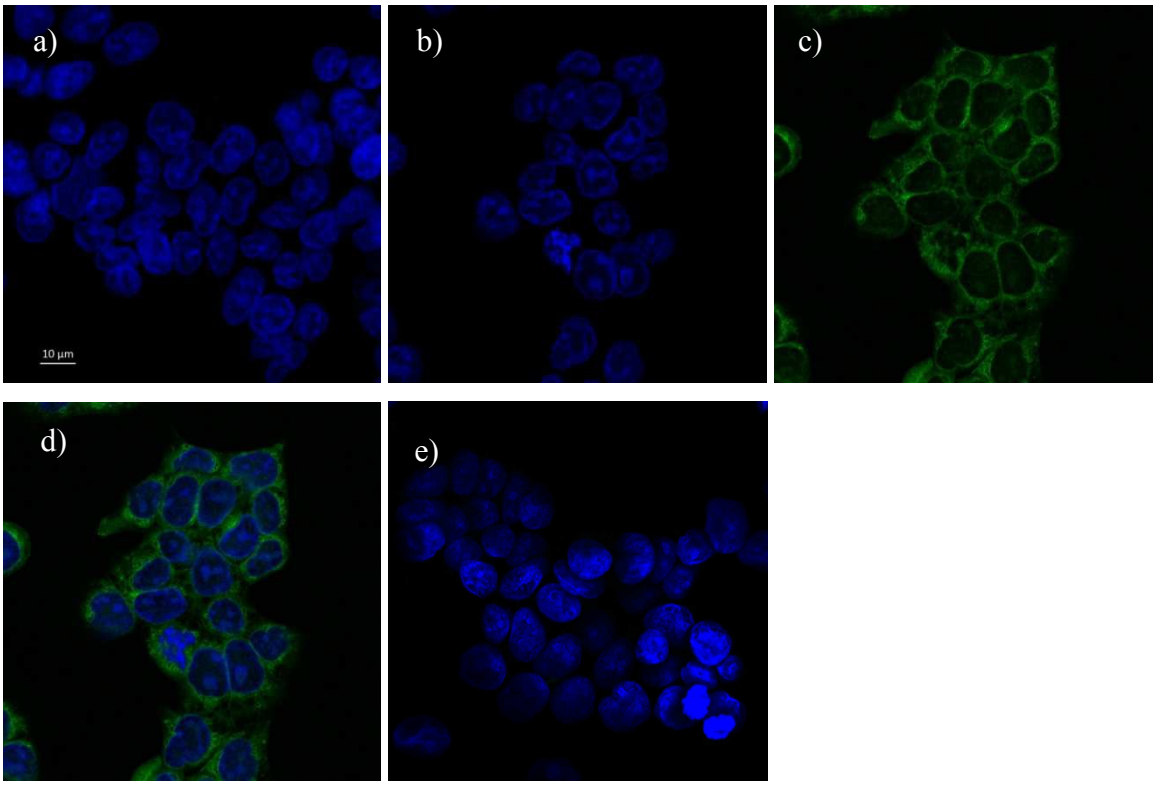

Figure 2. Fluorescence labeling of COX-2 expressing cells (HCA-7 cells): (**a**) Cells treated with PBS (control); (**b, c, d**) cells treated with 100 µM conjugate **6**; in figure **b**) the DAPI stained nucleus is shown only (perinuclear staining is not shown here); **(c)** represents perinuclear staining due to uptake of compound **6** in HCA-7 cells (nuclear staining is not shown here); **(d)** represents a merged image of both nuclei and perinuclear staining as a result of uptake of compound **6** in HCA-7 cells; (**e**) cells were treated with 5 µM celecoxib **1** before the incubation with compound **6**.

View Article Online
DOI: 10.1039/C6OB00493H

***Fluorescence imaging with COX-2-negative HCT-116 cells*:**

To determine whether the fluorescence labeling of HCA-7 with compound **6** depends on COX-2 isozyme expression or not, a fluorescence imaging experiment using HCT-116 (COX-2-negative human colon cancer) cells was performed. DAPI was used as nuclear stain. HCT-116 cells were incubated with compound **6** (100 or 500 μM) at 37 ^{o}C and cells were imaged by confocal microscopy.

No fluorescence labeling was observed at either concentration of compound **6** (Figure 3b, c), and no fluorescence labeling was observed after incubation with PBS control as expected (Figure 3a). The results of this experiment in COX-2-negative HCT-116 cells validated the hypothesis that the fluorescence labelling of HCA-7 colon cancer cells with compound **6** is due to COX-2 specific binding of fluorescence conjugate.

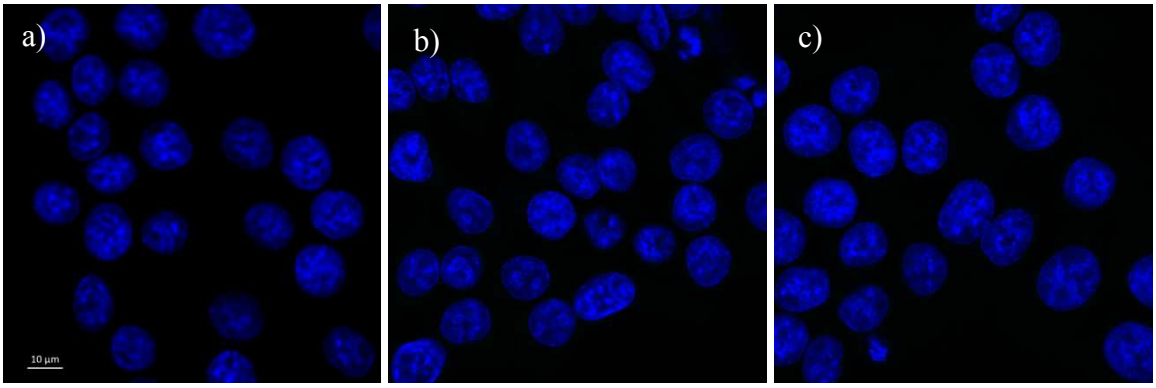

Figure 3. Uptake of compound **6** in HCT-116 cells: cells were treated with a) PBS (control), b) compound **6** at 500 μM concentration and c) compound **6** at 100 μM concentration.

View Article Online
DOI: 10.1039/C6OB00493H

CONCLUSIONS

A group of novel fluorescent conjugates have been synthesized, wherein a pyrimidine scaffold was coupled either directly or via linker to the NBD fluorophore. *In vitro* COX-1/COX-2 inhibition studies indicated that all three compounds are selective inhibitors of COX-2. Lead compound **6** was evaluated for fluorescent COX-2 visualization in human colon cancer cells. Fluorescence labelling experiments in HCA-7 cells and HCT-116 indicated that compound **6** is capable to label the COX-2 enzyme in human colon cancer cells. In contrast to earlier work, here we did not link the fluorophore to an "intact" anti-inflammatory drug, but rather attempted to transform our previously reported highly potent and efficient COX-2 radiotracer **3** into a fluorescent probe by replacing a part of the molecule with the fluorophore. The resulting compounds showed a substantial decline in COX-2 potency but lead compound **6** still showed success in selectively labelling COX-2 at a concentration of 100 μM. Future inquiry might look into attaching the NBD fluorophore at the methyl sulfone/sulfonamide moiety of an "intact" pyricoxib scaffold at achieve an improved activity and sensitivity profile.

View Article Online
DOI: 10.1039/C6OB00493H

MATERIALS AND METHODS

General

All reagents and solvents were obtained from Sigma-Aldrich, unless otherwise stated and used without further purification. Nuclear magnetic resonance spectra were recorded on a 600 MHz Burker unit. ^{1}H-NMR and ^{13}C-NMR chemical shifts are recorded in ppm relative to tetramethylsilane (TMS). ^{19}F-NMR chemical shifts are recorded in ppm relative to trichlorofluoromethane. Mass spectra were obtained using am Agilent Technologies 6220 oaTOF instrument. Column chromatography was conducted using Merck silica gel (mesh size 230–400 ASTM). Thin-layer chromatography (TLC) was performed on Merck silica gel F-254 aluminum plates, with visualization under UV light (254 nm).

Chemistry

2-(Methylsulfonyl)-4-(4-(methylsulfonyl)-phenyl)-6-(trifluoromethyl)pyrimidine (**4**) was prepared according to literature procedure.[27,31]

***N*-(*N*-Boc-aminopropyl)-4-[4-(methylsulfonyl)phenyl]-6-(trifluoromethyl)-pyrimidin-2-amine (5).** 2-(Methylsulfonyl)-4-(4-(methylsulfonyl)-phenyl)-6-(trifluoromethyl)pyrimidine (**4**) (100 mg, 0.26 mmol) was dissolved in 2 ml CH_3CN and *N*-Boc-propylenediamine (228 µl, 1.3 mmol) was added. The reaction mixture heated in a sealed tube at 140 ^{o}C for 2 h and cooled to room temperature thereafter. 20 ml of 1N HCl was added, the product extracted with 3 x 20 ml ethyl acetate and used without further purification. The product was obtained as a white solid (72 mg, 58 % yield). ^{1}H-NMR (600 MHz, $CDCl_3$): 1.38 (s, 9H, C(CH_3)$_3$); 1.72-1.76 (m, 2H, CH_2); 3.04 (s, 3H, SO_2CH_3); 3.19 (m, 2H, NHCH_2); 3.54-3.58 (m, 2H, NHCH_2); 4.90 (s, 1H, N*H*); 5.82 (s, 1H, N*H*); 7.19 (s, 1H, *H*-5 of pyrimidine); 8.01 (m, J = 8.4 Hz, 2H, sulfonylphenyl *H*-2, *H*-6); 8.16 (m, J = 8.4 Hz, 2H, sulfonylphenyl *H*-3, *H*-5). LR-MS: 497.2 [M+Na].

View Article Online
DOI: 10.1039/C6OB00493H

***N*-(2-((7-Nitrobenzo[c][1,2,5]oxadiazol-4-yl)amino)propyl)-4-[4-(methylsulfonyl)phenyl]-6-(trifluoromethyl)-pyrimidin-2-amine (6).** Trifluoroacetic acid (TFA) (50 µL, 0.65 mmol) was added to a solution of compound **5** (50 mg, 0.11 mmol) in dry CH_2Cl_2 (5 mL), and the reaction mixture was stirred at 25 °C for 6 h.

The progress of the reaction was monitored with TLC, upon completion excess acid and solvent was removed under vacuum, and the residue was dried in vacuo overnight. The deprotected product was dissolved in dry THF (2 mL) under a nitrogen atmosphere, without further purification, and a solution of NBD-Cl (20 mg, 0.10 mmol) in dry TEA (50 µL, 0.36 mmol) was added. The reaction was stirred at 25 °C for 1 h, H_2O added, and the mixture extracted with CH_2Cl_2 (3×10 mL). The combined organic extracts were washed with brine prior to drying over anhydrous Na_2SO_4. Solvent was removed in vacuo and the product was purified by column chromatography using a gradient of EtOAc/hexane running from 10% EtOAc to 50%. The product thus obtained was not of a sufficient purity to be taken forward into *in vitro* studies. Final purification was conducted using semi-preparative HPLC using an isocratic solvent mixture of 70/30 CH_3CN / H_2O, a flow rate of 3 ml/min on Phenomenex LUNA® C18 column (100 Å, 250 × 10 mm, 10 µm) and a Gilson 322 Pump module fitted with a 171 Diode Array detector. The product was obtained as a brown solid (15 mg, 25 % yield). ^{1}H-NMR (600 MHz, d_6-DMSO): 1.92-1.96 (m, 2H, CH_2); 3.26 - 3.30 (m, 2H, NHCH_2); 3.30 (s, 3H, SO_2CH_3); 3.58 - 3.62 (m, 2H, NHCH_2); 6.36 (d, J = 8.4 Hz, 1H, *H*-5 of NBD); 7.62 (s, 1H, *H*-5 of pyrimidine); 7.95 (d, J = 8.4 Hz, 2H, sulfonylphenyl *H*-2, *H*-6); 8.13 (d, J = 8.4 Hz, 2H, sulfonylphenyl *H*-3, *H*-5); 8.39 (d, J = 8.4 Hz, 1H, *H*-6 of NBD); 9.5 (s, 1H, N*H*). ^{19}F-NMR (560 MHz, d_6-DMSO): -69.1 (s, 3F, CF_3). ^{13}C NMR (d_6-DMSO, 150 MHz): δ: 28.08 (CH_2), 39.01 (CH_2), 39.09 (CH_2), 43.82 (CH_3), 101.94 (pyrimidine ArCH), 102.08 (NBD ArCH), 120.28 (q, $^1J_{C-F}$ = 275 Hz, CF_3), 127.93 (2 x ArCH of sulfonylphenyl), 128.64 (2 x ArCH of sulfonylphenyl), 130.10 (ArC), 138.17 (ArCH), 141.11 (NBD ArC), 143.42 (ArC), 144.42 (ArC), 144.84 (ArC), 145.63 (ArC), 156.94 (q, $^2J_{C-CF}$ = 36 Hz), 162.81 (pyrimidine ArC), 165.46 (pyrimidine ArC). HRMS (ESI) calculated for $C_{21}H_{18}F_3N_7O_5S$ $[M-H]^-$ 536.0964; found $[M-H]^-$ 536.0969.

View Article Online
DOI: 10.1039/C6OB00493H

***N*-(*N*-Boc-aminoethyl)-4-[4-(methylsulfonyl)phenyl]-6-(trifluoromethyl)-pyrimidin-2-amine (7).** 2-(Methylsulfonyl)-4-(4-(methylsulfonyl)-phenyl)-6-(trifluoromethyl)pyrimidine (**4**) (100 mg, 0.26 mmol) was dissolved in 2 ml CH_3CN and *N*-Boc-ethylenediamine (200 µl, 1.3 mmol) added. The reaction mixture heated in a sealed tube at 140 °C for 2 h and cooled to room temperature thereafter. 20 ml of 1N HCl were added, the product extracted with 3 x 20 ml ethyl acetate and used without further purification. The product was obtained as a white solid (76 mg, 64 % yield). ^{1}H-NMR (600 MHz, $CDCl_3$): 1.35 (s, 9H, $C(CH_3)_3$); 3.06 (s, 3H, SO_2CH_3); 3.34-3.38 (m, 2H, $NHCH_2$); 3.58-3.62 (m, 2H, $NHCH_2$); 4.9 (s, 1H, N*H*); 5.8 (s, 1H, N*H*); 7.23 (s, 1H, *H*-5 of pyrimidine); 8.01 (d, J = 8.4Hz, 2H, sulfonylphenyl *H*-2, *H*-6); 8.16 (d, J = 8.4Hz, 2H, sulfonylphenyl *H*-3, *H*-5). LR-MS: 483.1 [M+Na].

***N*-(2-((7-nitrobenzo[c][1,2,5]oxadiazol-4-yl)amino)ethyl)-4-[4-(methylsulfonyl)phenyl]-6-(trifluoromethyl)-pyrimidin-2-amine (8).**

Trifluoroacetic acid (TFA) (50 µL, 0.65 mmol) was added to a solution of compound **7** (50 mg, 0.11 mmol) in dry CH_2Cl_2 (5 mL), and the reaction mixture was stirred at 25 °C for 6 h. The progress of the reaction was monitored by TLC, upon completion excess acid and solvent was removed under vacuum, and the residue was dried in vacuo overnight. The deprotected product was dissolved in dry THF (2 mL) under a nitrogen atmosphere, without further purification, and a solution of NBD-Cl (20 mg, 0.10 mmol) in dry TEA (50 µL, 0.36 mmol) was added. The reaction was stirred at 25 °C for 1 h, H_2O added, and the mixture extracted with CH_2Cl_2 (3×10 mL). The combined organic extracts were washed with brine prior to drying over anhydrous Na_2SO_4. Solvent was removed in vacuo and the product purified by column chromatography using a gradient of EtOAc/hexane running from 10% EtOAc to 50%. The product thus obtained was not of a sufficient purity to be taken forward into *in vitro* studies. Final purification was conducted using semi-preparative HPLC using an isocratic solvent mixture of 70/30 CH_3CN / H_20, a flow rate of 3 ml/min on Phenomenex LUNA® C18 column (100 Å, 250 × 10 mm, 10 µm) and a Gilson 322 Pump module fitted with a 171 Diode Array detector. The product was obtained as a brown solid (10 mg, 17 % yield). ^{1}H-NMR (600 MHz, d_6-DMSO): 3.30 (s, 3H, SO_2CH_3); 3.30 - 3.34 (m, 2H, $NHCH_2$); 3.79 - 3.83 (m, 2H, $NHCH_2$); 6.57 (d, J = 8.4 Hz, 1H, *H*-5 of NBD); 7.69 (s, 1H, *H*-5 of pyrimidine); 7.91 (d, J = 8.4 Hz, 2H,

View Article Online
DOI: 10.1039/C6OB00493H

sulfonylphenyl *H*-2, *H*-6); 8.19 (d, J = 8.4 Hz, 2H, sulfonylphenyl *H*-3, *H*-5); 8.45 (d, J = 8.4 Hz, 1H, *H*-6 of NBD); 9.5 (s, 1H, N-*H*). ^{19}F-NMR (560 MHz, d_6-DMSO)): -69.09 (s, 3F, CF_3). ^{13}C NMR (d_6-DMSO, 150 MHz): δ: 43.01 (CH_3), 49.00 (CH_2), 49.46 (CH_2), 102.37 (pyrimidine ArCH), 102.73 (NBD ArCH), 121.62 (q, $^1J_{C–F}$ = 275 Hz, CF_3), 127.55 (2 x ArCH of sulfonylphenyl), 127.72 (2 x ArCH of sulfonylphenyl), 128.20 (ArC), 135.64 (ArCH), 140.89 (NBD ArC), 141.20 (ArC), 143.07 (ArC), 144.45 (ArC), 145.59 (ArC), 156.84 (q, $^2J_{C–CF}$ = 36 Hz), 159.94 (pyrimidine ArC), 165.63 (pyrimidine ArC). LR-MS: 546.1 [M+Na]. HRMS (ESI) calculated for $C_{20}H_{16}F_3N_7O_5S$ $[M-H]^-$ 522.0807; found $[M-H]^-$ 522.0816.

4-Amino-7-nitrobenzofurazan (9).

NBD-NH_2 was prepared according to literature procedure.[25] The product was obtained as a yellow solid (126 mg, 70 % yield). ^{1}H-NMR (600 MHz, $CDCl_3$): 5.60 (s, 2H, NH_2); 6.34 (d, J = 8.4 Hz, 1H, *H*-5 of NBD); 8.41 (d, J = 8.4 Hz, 1H, *H*-6 of NBD). LR-MS: 203.0 [M+Na].

***N*-(7-Nitrobenzo[c][1,2,5]oxadiazol-4-yl)-4-[4-(methylsulfonyl)phenyl]-6-(trifluoromethyl)-pyrimidin-2-amine (10).** 2-(methylsulfonyl)-4-(4-(methylsulfonyl)-phenyl)-6-(trifluoromethyl)pyrimidine (**4**) (50 mg, 0.13 mmol) and 4-amino-7-nitrobenzofurazan (**9**) were dissolved in 1 ml CH_3CN. The reaction mixture heated in a sealed tube at 140 ^oC for 2 h and cooled to room temperature thereafter. 10 ml of 1N HCl were added, the product extracted with 3 x 10 ml ethyl acetate and purified by column chromatography eluting at 30% EtOAc / hexane. The product was obtained as a yellow brownish solid (34 mg, 54% yield). ^{1}H-NMR (600 MHz, d_6-DMSO): 3.34 (s, 3H, SO_2CH_3); 8.17 (d, J = 8.4 Hz, 2H, sulfonylphenyl *H*-2, *H*-6); 8.40 (s, 1H, *H*-5 of pyrimidine); 8.43 (d, J = 8.4 Hz, 1H, *H*-6 of NBD); 8.65 (d, J = 8.4 Hz, 2H, sulfonylphenyl *H*-3, *H*-5); 8.90 (d, J = 8.4 Hz, 1H, *H*-5 of NBD); 11.83 (s, 1H, N*H*). ^{19}F-NMR (560 MHz, d_6-DMSO): -68.35 (s, 3F, CF_3). ^{13}C NMR (d_6-DMSO, 150 MHz): δ: 48.09 (CH_3), 108.48 (pyrimidine ArCH), 113.01(NBD ArCH), 121.10 (q, $^1J_{C–F}$ = 275 Hz, CF_3), 128.15 (2 x ArCH), 129.13 (ArC), 129.38 (2 x ArCH), 136.53 (NBD ArC), 136.60 (ArCH), 139.85 (NBD ArC), 144.06 (ArC), 144.15 (ArC), 146.31(ArC), 156.77 (q, $^2J_{C–CF}$ = 36.1 Hz), 159.64 (pyrimidine ArC), 166.45 (pyrimidine ArC). HRMS (ESI) calculated for $C_{18}H_{11}F_3N_6O_5S$ $[M-H]^-$ 479.0385; found $[M-H]^-$ 479.0392.

View Article Online
DOI: 10.1039/C6OB00493H

Cyclooxygenase inhibition assay

The ability of celecoxib (**1**) and new compounds (**6, 8** and **10)** to inhibit ovine COX-1 and recombinant human COX-2 was determined using a COX fluorescence inhibitor assay (Cayman Chemical, Ann Arbor, USA; catalog #: 700100) according to the manufacturers protocol. Compounds were assayed in a concentration range of 10^{-9} M to 10^{-3} M.

Cell culture and cell imaging studies

HCA-7 cells. HCA-7 colony 29 cells (Sigma Aldrich, 02091238) were used for fluorescence imaging of COX-2 over-expression. The cells were cultured in T75 flasks using DMEM/F12 (1:1) medium supplemented with 10% (v/v) fetal bovine serum (GIBCO, 12483), 2 mM L-glutamine (GIBCO, 25030), 1% penicillin/streptomycin and 20 mM HEPES buffer (GIBCO, 15630) and were kept in a 37°C humidified incubator with a supply of 5% CO_2 in air. After the cells were 80% confluent, they were harvested using 0.25% trypsin-EDTA (GIBCO, 25200) and plated onto sterilized glass cover slips placed into a 6 well cell culture plate at a density of 200,000 cells/well. Cells were washed twice using PBS prior to permeabilization with 0.5% Triton X-100 supplemented PBS (pH 7.4) for 5 min. Fixed and permeabilized cells were washed thrice with PBS before the addition of PBS as control, compound **6** (100 µM), or a mixture of 100 µM celecoxib and 100 µM compound **6** to the cover slips placed in a cell culture plate, respectively. This set up was placed for incubation at 37°C for 1 hour. Thereafter, the cells were washed with 0.1% Triton X-100 supplemented PBS followed by three washes with PBS. PBS rinsed coverslips were then mounted onto microscopy slides using 30 µL drops of poly vinyl alcohol based mounting media supplemented with 0.1% n-propyl gallate as anti-fade and DAPI (50 µg/ml).

Cells were imaged using corresponding lasers for visualizing DAPI (blue nuclear staining) and FITC (green emission) with a Plan-Apochromat 40X/1.3 Oil DIC M27 lens on a Zeiss LSM 710 AxioObserver confocal laser scanning microscope.

View Article Online
DOI: 10.1039/C6OB00493H

HCT-116 cells. HCT-116 cells (ATCC) were cultured at 37°C in a humidified atmosphere of 5% (v/v) CO_2, using DMEM/F12 medium supplemented with 10% fetal bovine serum (FBS) (Gbico®), 2mM L-glutamine (Invitrogen) and 1% antibiotic/antimycotic (Invitrogen). Cell growth medium was changed every other day. Cells were treated with 0.25% Trypsin/1mM EDTA (Invitogen) for about 5 min at room temperature to dissociate from the culture flask, and rinsed with PBS once after harvesting. Cells were resuspended in fresh growth medium and seeded to the 6-well plate at $1.5x10^6$ cells per well. After removing media, cells were treated with 100 μM and 500 μM of compound **6** respectively using the procedure mentioned above.

ACKNOWLEDGMENTS

The authors would like to acknowledge the Dianne and Irving Kipnes Foundation, the Canadian Institute for Health Research (CIHR and the National Science and Engineering Research Council of Canada (NSERC) for supporting this work. F.W. and J.K. thank the Alberta Cancer Foundation (ACF) for a postdoctoral fellowship.

View Article Online
DOI: 10.1039/C6OB00493H

REFERENCES

1. Hanahan, D.; Weinberg, R. *Cell*. **2011**, 144, 646674.
2. Mantovani, A.; Allavena, P.; Sica, A.; Balkwill, F. *Nature*. **2008**, 454, 436.
3. Scheiman, J. M. *Drugs*. **2006**, 66, 15.
4. Seibert, K.; Zhang, Y.; Leahy, K.; Hauser, S.; Masferrer, J.; Perkins, W.; Lee, L.; Isakson, *P. Proc. Natl. Acad. Sci. U S A.* **1994**, 91, 12013.
5. Marnett, L. J. *Annu. Rev. Pharmacol. Toxicol.* **2009**, 49, 265.
6. Rao, P. P. N.; Kabir, S.N.; Mohamed T. *Pharmaceuticals*, **2010**, *3*, 1530.
7. Rao, P. P. N.; Chen, Q.-H.; Knaus, E. E. *J. Med. Chem.* **2006**, *49*, 1668.
8. Bhardwaj, A.; Huang, Z.; Kaur, J.; Knaus, E. E. *ChemMedChem* **2012**, 7, 62.
9. Edwards, J.; Mukherjee, R.; Munro, A.F.; Wells, A.C.; Almushatat, A.; Bartlett, J. M. S. *Eur. J. Cancer*. **2004**, 40, 50.
10. Wang, D.; DuBois, R.N. *Oncogene*. **2010**, 29, 781.
11. Jiménez, P.; García, A.; Santander, S.; Piazuelo, E. *Curr. Pharm. Des*. **2007**, 13, 2261.
12. Méric, J.; Rottey, S.; Olaussen, K.; Soria, J.; Khayat, D.; Rixe, O.; et al. *Crit. Rev. Oncol*. **2006**, 59, 51.
13. Singh, P.; Bhardwaj, A. *J. Med. Chem*. **2010**, 53, 3707.
14. Kismet, K.; Akay, M. T.; Abbasoglu, O.; Ercan, E. *Cancer Detect. Prev*. **2004**, 28, 127.
15. Pommery, N.; Taverne, T.; Telliez, A.; Goossens, L.; Charlier, C.; Pommery, J.; Goossens, J. F.; Houssin, R.; Durant, F.; Henichart, J.-P. *J. Med. Chem*. **2004**, 47, 6195.
16. Chan, T. A. *Lancet Oncol*. **2002**, 3, 166.
17. Howe, L. R. Breast *Cancer Res.* **2007**, 9, 210.
18. Giovannucci, E.; Rimm, E.; Stampfer, M.; Colditz, G.; Ascherio, A.; Willett, W. *Ann. Intern. Med*. **1994**, 121, 241.
19. Tietz, O.; Marshall, A.; Wuest, M.; Wang, M.; Wuest, F. *Curr. Med. Chem*. **2013**, 20, 4350.
20. Pacelli, A.; Greenman, J.; Cawthorne, C.; Smith, G. *J. Labelled Compd. Radiopharm*. **2014**, 57, 317.
21. Laube, M.; Kniess, T.; Pietzsch, J. *Molecules*. **2013**, 18, 6311.
22. Thomas, J.A. *Chem. Soc. Rev*. **2015**, 44, 4494.
23. Wysocki, L.M.; Lavis, L.D. *Curr. Opin. Chem. Biol*. **2011**, 15, 752.

View Article Online
DOI: 10.1039/C6OB00493H

24. Uddin, M. J.; Crews, B. C.; Blobaum, A. L.; Kingsley, P. J.; Gorden, D. L.; McIntyre, J. O.; Matrisian, L. M.; Subbaramaiah, K.; Dannenberg, A. J.; Piston, D. W.; Marnett, L. J.; *Cancer Res*. **2010**, 70, 3618.
25. Bhardwaj, A.; Kaur, J.; Sharma, S. K.; Huang, Z.; Wuest, F.; Knaus, E. E. *Bioorg. Med. Chem. Lett.* **2013**, 23, 163.
26. Uddin, M. J.; Crews, B. C.; Huda, I.; Ghebreselasie, K.; Daniel, C. K.; Marnett, L. J. *ACS Med. Chem. Lett.* **2014**, 5, 445-450
27. Bhardwaj, A.; Kaur, J.; Wuest, F.; Knaus, E. E. *ChemMedChem*. **2014**, 9, 109.
28. Tietz, O.; Sharma, S.K.; Kaur, J.; Way, J.; Marshall, A.; Wuest, M.; Wuest, F. *Org. Biomol. Chem*. **2013**, 11, 8052.
29. Kaur, J.; Tietz, O.; Bhardwaj, A.; Marshall, A.; Way, J.; Wuest, M.; Wuest, F. *ChemMedChem* **2015**, 10, 1635.
30. Tietz, O.; Dzandzi, J.; Bhardwaj, A.; Valliant, J.; Wuest, F. *Bioorg. Med. Chem. Lett.* **2016**, 26, 1516.
31. Swarbrick, M.; Beswick, P.; Gleave, R.; Green, R.; Bingham, R.; Bountra, C.; et al. *Bioorg. Med. Chem. Lett*. **2009**, 19, 4504.